JOURNAL OF NANO- AND ELECTRONIC PHYSICS
Vol. 12 No 3, 03014(5pp) (2020)
ЖУРНАЛ НАНО- ТА ЕЛЕКТРОННОЇ ФІЗИКИ
Том 12 № 3, 03014(5cc) (2020)

Electric Properties of MCM-41 <$SmCl_3$> Nanohybrid Encapsulate

Fedir Ivashchyshyn[1,2,*], Dariusz Calus[1], Anna Pidluzhna[2], Piotr Chabecki[1]

[1] *Czestochowa University of Technology, Faculty of Electrical Engineering, 17, Al. Armii Krajowej, 42200 Częstochowa, Poland*
[2] *Lviv Polytechnic National University, 12, Bandera St., 79013 Lviv, Ukraine*

(Received 14 January 2020; revised manuscript received 20 June 2020; published online 25 June 2020)

Probably the most popular compound for the synthesis of complex hybrid structures especially during the last decade is a molecular silica matrix MCM-41. Many different classes of substances were obtained on its bases. Samarium is a well-known magnetic material and its salts are widely used in laboratories for research on new compounds of samarium. Therefore, we decided to insert the samarium-containing compound into MCM-41 matrix and investigate its electric properties from the perspective of magneto- and photosensitive applications. The samarium (III) chloride $SmCl_3$ placed in mesoporous silica matrix MCM-41 with use of encapsulation technique was successfully synthesised. Electric properties of obtained nanohybrid encapsulate were investigated using impedance spectroscopy method. The character of impedance frequency dispersion, loss tangent and permittivity of MCM-41 <$SmCl_3$> synthesized material in darkness, under illumination and in magnetic field were determined. The thermogalvanic effect was observed and its mechanisms were analyzed. The observed magneto- and photoinduced negative capacitance effects for obtained MCM-41 <$SmCl_3$> nanohybrid opens up the possibilities for its application in nongyrator delay nanolines with optically and magnetically operable parameters.

Keywords: Mesoporous MCM-41 matrix, Impedance spectroscopy, Nyquist plot, Dielectric permittivity, Loss tangent, Thermogalvanic effect.

DOI: 10.21272/jnep.12(3).03014 PACS numbers: 74.25.nn, 81.05.Rm

1. INTRODUCTION

An interesting approach to technology for nonelectrochemical energy generators was enabled by a discovery of a notable phenomenon described in works of Kaminskii et al. [1, 2]. The electromotive force EMF was generated in SmS defect crystal structure during heating-up in the absence of extrinsic temperature gradients. The value for EMF generated in 1.3 s impulse was 2.5 V [1] and 0.6 V in continuous regime [2]. The following works in the area were dedicated to spontaneous generation of EMF at ambient temperature in ZnO [3-5] doped with impurities of different valence but the EMF value was in the millivolt range.

As it was determined in [1, 6], the local defects were the reason for EMF generation phenomenon in SmS. The proposed model for EMF generation let assume the possibility to observe the same phenomenon in other semiconductor substances. The necessary requirement for observation of this EMF generation effect is the presence of nonequilibrium distribution of donor impurity of concentration high enough in a bulk. For example, the EMF generation effect was observed in $Sm_{0.99}Gd_{0.01}S$ and $SmTe_xS_{1-x}$, where $x = 0.02$ and 0.05 under constant heating [7].

Therefore, the purpose of our work was to investigate the above-stated assumption and supramolecular compound of complex structure based on silicate matrix MCM-41 and $SmCl_3$ was synthesised. The developed approach could help to understand the nature of EMF generation phenomenon and develop the methods for its improvement.

2. EXPERIMENTS AND METHODS

MCM-41 molecular sieve structure based on SiO_2 was chosen as the initial matrix for supramolecular compound synthesis [8]. It is of hexagonal structure with walls of 0.6-0.8 nm in thickness. The MCM-41 initial matrix with pore size of ~ 37 Å and 984 m²/g specific surface area was used in our experiments. $SmCl_3$ was selected as the guest component because of its magnetic properties.

The method of encapsulation, described in [9, 10], was used for supramolecular structure formation. The electrical properties of the synthesised compound were investigated by means of impedance spectrometry (potentiostat/galvanostat 30 AUTOLAB, ECO CHEMIE). The measurement equipment is supplied with FRA-2 module and GPES software. The preliminary analysis of impedance data was made with Dirichlet filter [11, 12], and the following procedure for frequency dependent complex impedance was made by graphical analytical method with the ZView 2.3 (Scribner Associates) software. Inaccuracies of approximation did not exceed 4 %. The adequacy of equivalent models to the package of experimental data was confirmed by random character of residual first order differences for frequency dependences [11, 12].

Impedance investigations were executed in $10^{-3} \div 10^6$ Hz frequency range in ambient atmosphere, in an applied 2.75 kOe magnetic field and under illumination with 65 W solar imitator.

The spectra of thermostimulated discharge currents and spontaneously generated EMF were recorded during heating the sample up with 5 degree per minute increase in temperature.

* FedirIvashchyshyn@gmail.com

3. RESULTS AND DISCUSSION

The fine powder material of MCM-41 <$SmCl_3$> nanohybrid was successfully synthesised. The pellets of 2.5 mm in thickness and 5 mm in diameter were formed and electrical contacts were applied from the both sides of pellets.

The electrical resistivity of as formed pellets was investigated by means of impedance spectroscopy. The frequency f dependence of the real part of the complex impedance ReZ for synthesised MCM-41<$SmCl_3$> measured at normal conditions, at illumination and under applied magnetic field are presented in Fig. 1, and the specific resistance is close to 10^{10} Ohm·cm. The real part of the complex impedance ReZ for initial MCM-41 matrix is a monotonically decreasing value with a frequency dependent character (inset in Fig. 1) in whole frequency range. On the other hand, the insertion of $SmCl_3$ into MCM-41 leads to specific resistance decrease by three orders with simultaneous change in ReZ behaviour with frequency. The real part of the complex impedance ReZ became frequency independent in $10^{-3}÷10^{3}$ Hz region and is shown in Fig. 1 (plot 1). The insertion of a guest component into initial matrix results in obvious and significant change in impurity energy band. The slight decrease in specific resistance is also observed under applied magnetic field (plot 2, Fig. 1). The nonmonotonic change in ReZ in low frequency region attracts ones attention and reaches the minimum near at $7·10^{-3}$ Hz. Such behaviour serves as an illustration for increase in conductivity as a result of charge carriers' delocalisation at the narrow band of attachment levels. Contrary to the MCM-41 <$SmCl_3$> behaviour in a magnetic field, the illumination of pellet of synthesised sample with white light provokes an increase in ReZ (plot 3, Fig. 1). The frequency dependence of ReZ is of abnormal character with an increase in specific resistance in low frequency region and its maximum at $5·10^{-2}$ Hz. At the same time, there are ReZ oscillations in a middle frequency region which could be initiated by charge carriers capturing and release by trap centres during time commensurable to half-period of sinusoidal signal of initial excitement. Hence, the illumination activates the trap states intensively and they capture and keep charge carriers then.

Interesting results can be observed during analysis of frequency dependence of the imaginary part of the complex impedance – ImZ. It should be mentioned that a well defined maximum for – ImZ appears near $1.5·10^4$ Hz for MCM-41 <$SmCl_3$> (plot 1, Fig. 2) which does not appear for initial MCM-41 matrix (inset in Fig. 2). The application of magnetic field and illumination leads to maxima shift to low-frequency region. Thus, at the constant magnetic field the maximum is observed near $6·10^3$ Hz (plot 2, Fig. 2) and under illumination maximum appears at $1.2·10^3$ Hz (plot 3, Fig. 2). The shift in maxima positions corroborates the redistribution of density of states above and under Fermi level that results in activation of additional deep trap centres.

The Nyquist plot for initial matrix MCM-41 is of classical character with two well defined arcs which represent charge transfer stages through the matrix itself and through the inter grain boundary (Fig. 3a). Such impedance character can be represented by two parallel $R||C$ units linked in series (1st equivalent electric circuit in Fig. 4). The Nyquist plot for MCM-41 <$SmCl_3$> nanohybrid structure consists of two arcs as well but they do not have a clear shape, and the low-frequency component appears as a line (Fig. 3b). The last feature of Nyquist plot can be modelled by the BCPE (Boundary Constant Phase Element) (2nd equivalent electric circuit in Fig. 4), which represents conductivity in spatially limited regions with complex conductivity [12]. The impedance behaviour of synthesised compound in a constant magnetic field demonstrates the negative capacitance effect with transfer to the 4th quadrant of complex plane.

This phenomenon can be caused by Zeeman effect. The same impedance behaviour appears under illumination but in a middle frequency region. In the last case, the mechanism of photoinduced negative capacitance most likely is related to electron excitation by light-wave from occupied states under Fermi level and trap centre formation for injected electrons. The relaxation time for these centres is longer than the half-period of sinusoidal initial signal. In general, this effect is well known in literature [13, 14] and comprehensively studied in works [15-17]. Therefore, the equivalent electric circuit for the last case contains inductive element L (3rd equivalent electric circuit in Fig. 4).

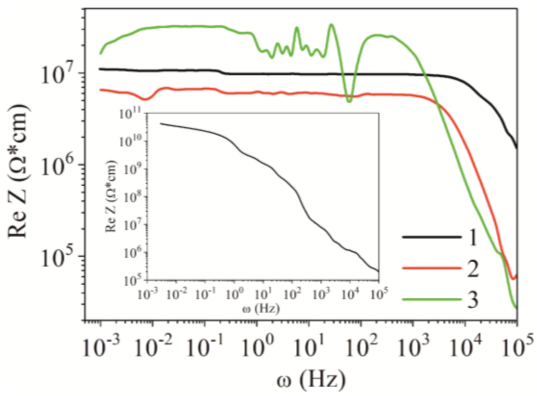

Fig. 1 – Frequency dependent real component of the specific complex impedance Z measured for MCM-41 <$SmCl_3$> under normal conditions (plot 1), in magnetic field (plot 2) and under illumination (plot 3). The inset shows the frequency dependent real component of the specific complex impedance Z measured for the initial MCM-41 matrix

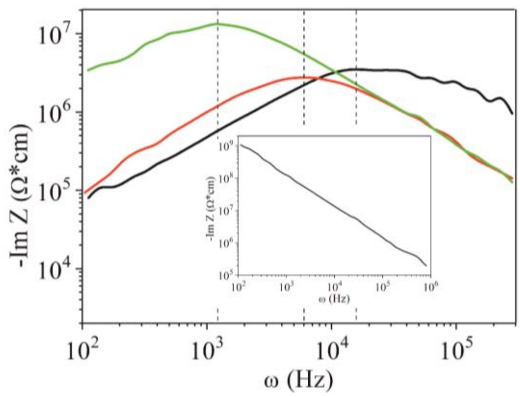

Fig. 2 – Frequency dependent imaginary part of the specific complex impedance Z measured for MCM-41 <$SmCl_3$> under normal conditions (plot 1), in magnetic field (plot 2) and under illumination (plot 3). The inset shows the frequency dependent real component of the specific complex impedance Z measured for the initial MCM-41 matrix

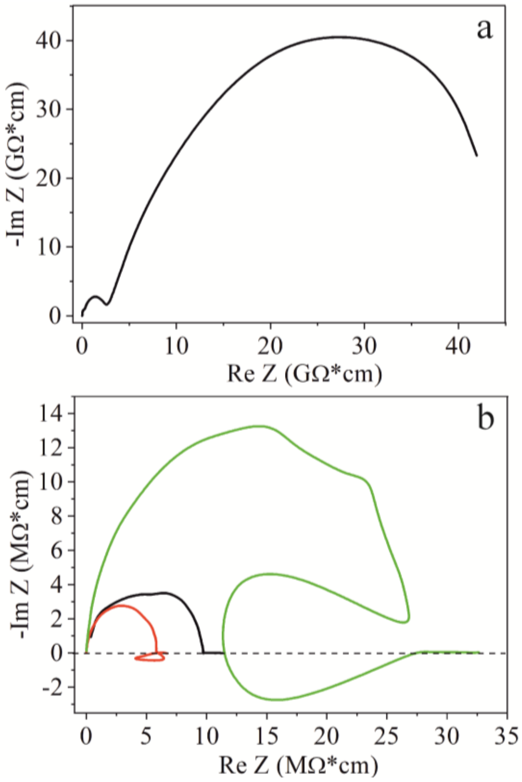

Fig. 3 – Nyquist plots for initial MCM-41 matrix (a) and nanohybrid MCM-41 <$SmCl_3$> (b) measured under normal conditions (plot 1), in magnetic field (plot 2) and under illumination (plot 3)

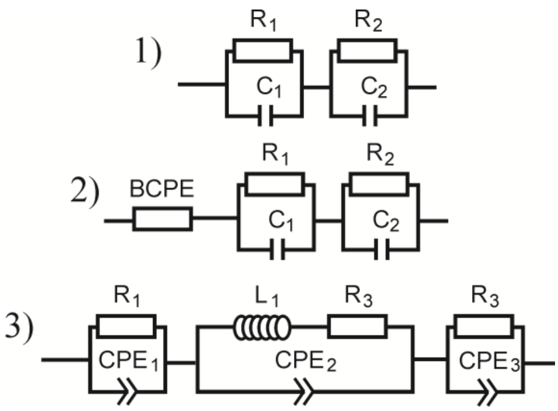

Fig. 4 – Equivalent electric circuits for Nyquist plots from Fig. 3 where *R* is the resistance, *C* is the capacitance, *L* is the inductance, CPE is the Constant Phase Element, BCPE is a finite Boundary Constant Phase Element

Constant phase element CPE of capacitive character models distributed capacitance [11] caused by vacancies or impurity defects, which provide electron conductivity at ambient temperature. It is noteworthy that observed effect can have a practical impact on development of magnetically and optically operated nanoscale gyrator-free delay lines.

The measurements of thermostimulated discharge spectrum (Fig. 5) serve as an evidence for statements described above. As seen from Fig. 5, the spectrum consists of narrow bands with a considerably higher density of levels and has well defined miniband character. The observable homo- and heterocharge relaxation process is important as well.

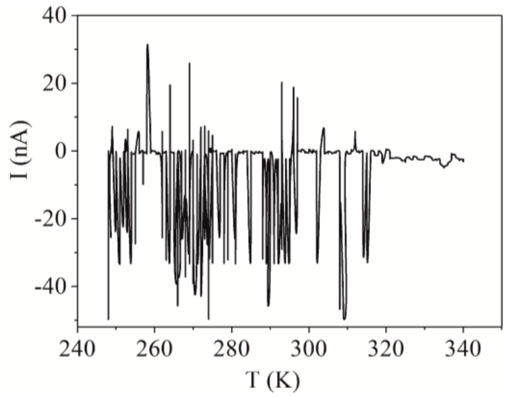

Fig. 5 – Thermostimulated discharge characteristic measured for MCM-41 <$SmCl_3$>

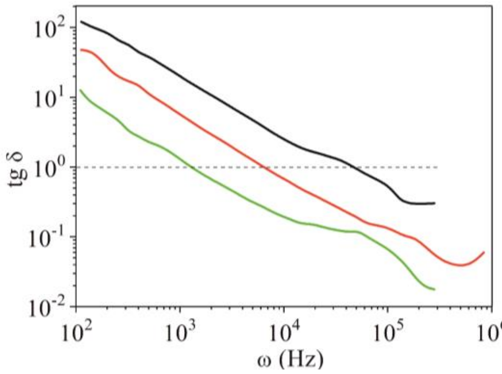

Fig. 6 – Frequency dependent loss tangent tgδ measured for MCM-41 <$SmCl_3$> under normal conditions (plot 1), in magnetic field (plot 2) and under illumination (plot 3)

The fact that peculiarities of MCM-41 <$SmCl_3$> energy structure will become apparent in polarisation properties is also obvious.

Dielectric properties of MCM-41 <$SmCl_3$> were investigated in a frequency range where loss tangent is less than unit (Fig. 6) with accentuation on advisability of the nanohybrid compound application. The dielectric permittivity of MCM-41 <$SmCl_3$> demonstrates an abnormal behaviour in a high frequency range (Fig. 7) but the maximum value is low anyway and does not make the compound practically attractive. However, the external field application leads to a giant increase in dielectric permittivity. The values for magnetic and capacitive effects are $\rho_H = 2800$ % and $\rho_L = 7700$ %, respectively, where ε_H is the dielectric permittivity in constant magnetic field, ε_L is the dielectric permittivity under illumination and ε_0 is the dielectric permittivity under normal conditions.

The obtained results confirm the advisability of development of obtained nanohybrid structure. It can be applied for highly magneto- and photosensible varicape that enables the switch from resistive sensors to capacitive analogues.

The magnetically and optically sensitive dielectric properties of MCM-41 <$SmCl_3$> became the reason to continue investigation in the direction of spontaneously generated EMF under constant heating. The temperature dependence of EMF is presented in Fig. 8. The maximum value for EMF is 10 mV and it makes nanostructured MCM-41 <$SmCl_3$> an attractive material for nonelectrochemical EMF generators.

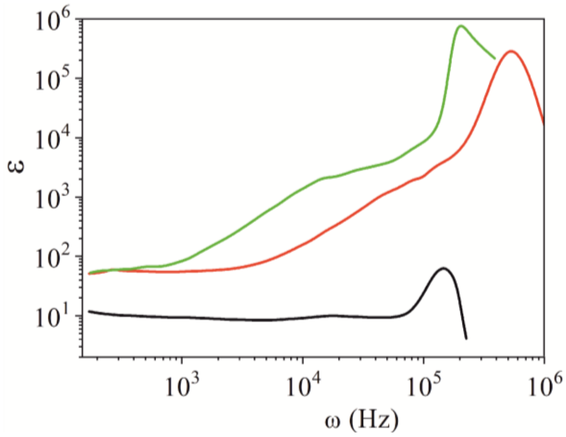

Fig. 7 – Frequency dependent permittivity ε measured for MCM-41 <$SmCl_3$> under normal conditions (plot 1), in magnetic field (plot 2) and under illumination (plot 3)

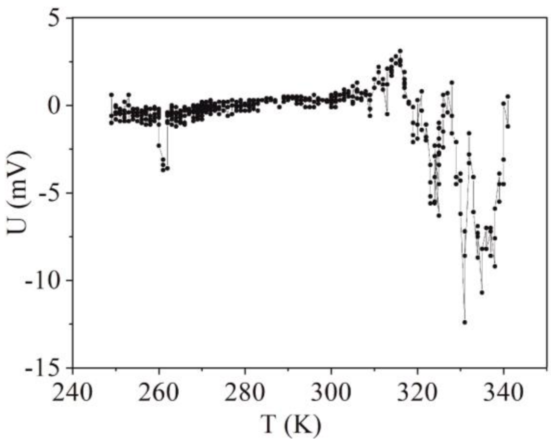

Fig. 8 – Spectrum of spontaneously generated EMF in MCM-41 <$SmCl_3$>

4. CONCLUSIONS

1. The encapsulation of samarium (III) chloride in MCM-41 matrix results in dielectric permittivity increase by three orders of magnitude, changes the behaviour of the real Re and imaginary Im components of the complex impedance *Z*.

2. The observed magneto- and photoinduced negative capacitance effects for obtained MCM-41 <$SmCl_3$> nanohybrid opens up the possibilities for its application in nongyrator delay nanolines with optically and magnetically operable parameters.

3. The giant magneto- and photocapacitive effects appear in MCM-41 <$SmCl_3$> encapsulate with the corresponding values ρ_H = 2800 %, ρ_L = 7700 % that makes it a promising alternative for exchange the resistive sensors of magnetic field onto capacitive analogues.

4. The encapsulation of samarium (III) chloride in MCM-41 matrix results in spontaneous generation of EMF of 10 mV in obtained compound under heating.

REFERENCES

1. V.V. Kaminskii, S.M. Solov'ev, *Phys. Solid State* **43**, 439 (2001).
2. V.V. Kaminskii, M.M. Kazanin, *Tech. Phys. Lett.* **34**, 361 (2008).
3. I.A. Pronin, D.T. Dimitrov, L.K. Krasteva, K.I. Papazova, I.A. Averin, A.S. Chanachev, V.A. Moshnikov, *Sensor. Actuat. A: Phys.* **206**, 88 (2014).
4. I.A. Pronin, B.V. Donkova, D.T. Dimitrov, I.A. Averin, J.A. Pencheva, V.A. Moshnikov, *Semiconductors* **48**, 842 (2014).
5. L.K. Krasteva, D.T. Dimitrov, K.I. Papazova, N.K. Nikolaev, T.V. Peshkova, V.A. Moshnikov, I.E. Gracheva, S.S. Karpova, N.V. Kaneva, *Semicoductors* **47**, 586 (2013).
6. V.V. Kaminskii, L.N. Vasil'ev, M.V. Romanova, S.M. Solov'ev, *Phys. Solid State* **43**, 1030 (2001).
7. V.V. Kaminskii, A.V. Golubkov, L.N. Vasil'ev, *Phys. Solid State* **44**, 1574 (2002).
8. M. Elhabiri, A.-M. Albrecht-Gary, *Coord. Chem. Rev.* **252**, 1079 (2008).
9. S.V. Baryshnikov, E.V. Charnaya, A.Y. Milinskii, E.V. Stukova, C. Tien, D. Michel, *Phys. Solid State* **52**, 392 (2010).
10. X. Guo, M. Lai, Y. Kong, W. Ding, Q. Yan, C.T.P. Au, *Langmuir* **20**, 2879 (2004).
11. Z.B. Stoynov, B.M. Grafov, B.S. Savova-Stoynova, V.V. Elkin, *Elektrokhimicheskii impedans (The Electrochemical Impedance)* (Moskov: Nauka Publishing House: 1991) [In Russian].
12. *Impedance Spectroscopy: Theory, Experiment, and Applications, 2nd Edition* (Eds. by E. Barsoukov, J.R. Macdonald) (Canada: Wiley Interscience: 2005).
13. J. Bisquert, H. Randriamahazaka, G. Garcia-Belmonte, *Electrochim. Acta* **51**, 627 (2005).
14. I. Mora-Sero, J. Bisquert, F. Fabregat-Santiago, G. Garcia-Belmonte, *Nano Lett.* **6**, 640 (2006).
15. F. Ivashchyshyn, I. Grygorchak, P. Stakhira, V. Cherpak, M. Micov, *Curr. Appl. Phys.* **12**, 160 (2012).
16. Tomasz Popławski, Anna Pidluzhna, Fedir Ivashchyshyn, Piotr Chabecki, Roman Shvets, *J. Nano- Electron. Phys.* **11** No 6, 06023 (2019).
17. P. Kostrobij, I. Grygorchak, F. Ivashchyshyn, B. Markovych, O. Viznovych, M. Tokarchuk, *J. Phys. Chem. A* **122**, 4099 (2018).

Електронні властивості наногібридного капсуляту MCM-41 <$SmCl_3$>

Fedir Ivashchyshyn[1,2], Dariusz Calus[1], Anna Pidluzhna[2], Piotr Chabecki[1]

[1] *Czestochowa University of Technology, Faculty of Electrical Engineering, 17, Al. Armii Krajowej, 42200 Częstochowa, Poland*

[2] *Lviv Polytechnic National University, 12, Bandera St., 79013 Lviv, Ukraine*

Імовірно, протягом останнього десятиріччя особливо, найбільш популярною сполукою для синтезу комплексних гібридних структур є молекулярна силікатна матриця MCM-41. Багато різноманітних класів сполук було отримано на її основі. Самарій є добре відомим металом завдяки своїм магнітним властивостям, та його солі широко використовуються в лабораторіях для синтезу нових сполук. Саме завдяки згаданим властивостям в даній роботі вирішено впровадити самарій-вмісну сполуку в матрицю MCM-41 та дослідити електричні властивості отриманого гібридного комплексу з точки зору його застосування в магнітному та оптичних полях. Впровадження самарій хлориду $SmCl_3$ в матрицю MCM-41 було успішно реалізовано з використанням методу інкапсулювання. Електричні властивості одержаного наногібридного інкапсуляту досліджено методом імпедансної спектроскопії та встановлено характер частотної дисперсії імпедансу, визначено тангенс кута втрат та діелектричну проникність MCM-41 <$SmCl_3$> в темряві, при освітленні та прикладеному ззовні магнітному полі. В синтезованій субстанції було досліджено термогальванічний ефект та проаналізовано його механізми. Зафіксована магнето- та фотоіндукована від'ємна ємність відкриває можливість застосування одержаної сполуки в безгіраторних нанолініях затримки з оптично та магнітно керованими параметрами.

Ключові слова: Нанопориста матриця MCM-41, Імпедансна спектроскопія, Діаграми Найквіста, Діелектрична проникність, Тангенс кута електричних втрат, Термо-ЕРС.